

Design and Implementation of Piezoelectric Transducer Driving System with MPPT and ZVS Features

Yu-Kai Chen, Chau-Chung Song and Chih-Ying Chen

Department of Aeronautical Engineering, National Formosa University
Hu-Wei, Yunlin 632, Taiwan, R.O.C.
E-mail: ykchen {at} nfu.edu.tw

ABSTRACT--- *This paper presents piezoelectric transducer driving system with maximum power point tracking (MPPT) and zero voltage switching (ZVS) features. The proposed driver is applied to ultrasonic cleaner and to achieve a good cleaning performance by varying the resonance frequency of piezoelectric transducer. The resonant frequency of piezoelectric transducer depends on the operating time, temperature and load. The piezoelectric driving system which includes half-bridge inverter, series resonant parallel loaded (SRPL) and an EM78P458 micro-controller. The driving system is done at a resonant frequency at which the electric impedance is minimum and the phase shift between the voltage and current of the transducer is nearly zero. For switching frequency $f_s >$ resonance frequency f_r , the phase shift $\varphi > 0$, the resonant tank represents an inductive load, thus the switches can be operated in ZVS. The measured results of the system are shown to verify the MPPT and ZVS features of the proposed system.*

Keywords--- piezoelectric 、 resonant tank 、 MPPT

1. INTRODUCTION

Ultrasonic cleaner uses ultrasound traveling through liquid to remove contaminants and deposits from material surfaces, holes, and cracks. Usually, piezoelectric transducer (PZT) is adopted as the vibration sources for the ultrasonic cleaner. The electrical performance of the piezoelectric transducer is depended on several factors e.g. mechanical load, temperature and deposits of polymer on the transducers [1]-[3]. A lot of inverter topologies and control methods for the PZT driving systems are found in the literature [4]-[10].

This paper presents a piezoelectric transducer driving system with maximum power point tracking (MPPT) and zero voltage switching (ZVS) features. The proposed driver is applied to ultrasonic cleaner and to achieve maximum cleaning performance by varying the resonant frequency of piezoelectric transducer.

2. SYSTEM CONFIGURATION AND DESIGN PROCEDURE

The piezoelectric driving system which includes half-bridge inverter, series resonant parallel loaded (SRPL) and an EM78P458 micro-controller. The control block diagram of the proposed ultrasonic cleaner system is shown in Fig. 1. To achieve the MPPT and ZVS features, the phases of the voltage and current of the piezoelectric transducer are sensed to determine the switching frequency of the half-bridge series resonant parallel loaded inverter (SRPLI). Fig. 2 shows the circuit of the SRPLI.

At the resonance frequency f_r and anti-resonance frequency f_a of the transducer, the impedance presented by the load is resistive. When the system frequency is between resonance frequency f_r and anti-resonance frequency f_a , it is inductive. Otherwise, the transducer is presented in capacitive. Resonance frequency f_r and anti-resonance frequency f_a are represented in equations (1) and (2).

$$f_r = \frac{1}{2\pi\sqrt{L_m C_m}} \quad (1)$$

$$f_a = \frac{1}{2\pi\sqrt{\frac{L_m C_m C_b}{C_m + C_b}}} \quad (2)$$

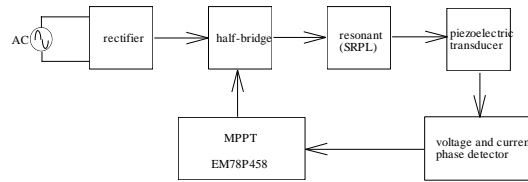


Fig. 1. The control block diagram of an ultrasonic cleaner system.

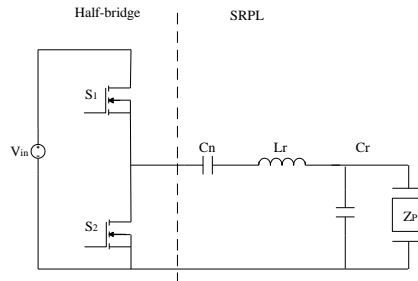


Fig. 2. Half-bridge SRPLI driving circuit for an ultrasonic cleaner system.

The driving system is done at a resonant frequency at which the electric impedance is minimum, and the phase shift between the voltage and current of the transducer is nearly zero.

The resonance frequency of piezoelectric transducer depends on its time, temperature and load. The piezoelectric driving system which includes half-bridge inverter, SRPLI and an EM78P458 micro-controller.

The design criterions and procedure of the proposed system are listed as follows:

1. The transducer all operates at resonance frequency for the best clean performance,
2. The SRPLI all operates in inductive load for zero voltage switching (ZVS) feature.

Step 1 :

Determine the value of resonance inductor L_r and capacitor C_r , using (3)

$$\frac{|V_{ZP}|}{|V_{in}|} = \frac{\sqrt{2}V_I}{\pi} \times \frac{1}{\sqrt{\left[1 - \left(\frac{\omega_s}{\omega_o}\right)^2\right]^2 + \left(\frac{\omega_s}{\omega_o Q}\right)^2}} \quad (3)$$

where : ω_s switching frequency, ω_o : natural frequency = $\frac{1}{\sqrt{L_r C_r}} = 2\pi f_o$,

and quality factor $Q := \frac{R_m}{\sqrt{\frac{L_m}{C_m}}}$.

Step 2:

For switching frequency $f_s >$ resonant frequency f_r , the phase shift $\phi > 0$, the resonant tank represents an inductive load, thus the switches can be operated in ZVS. Thus, we can determine the switching frequency. The key waveforms of the SRPLI when the system is operated under inductive load which are shown in Fig. 3.

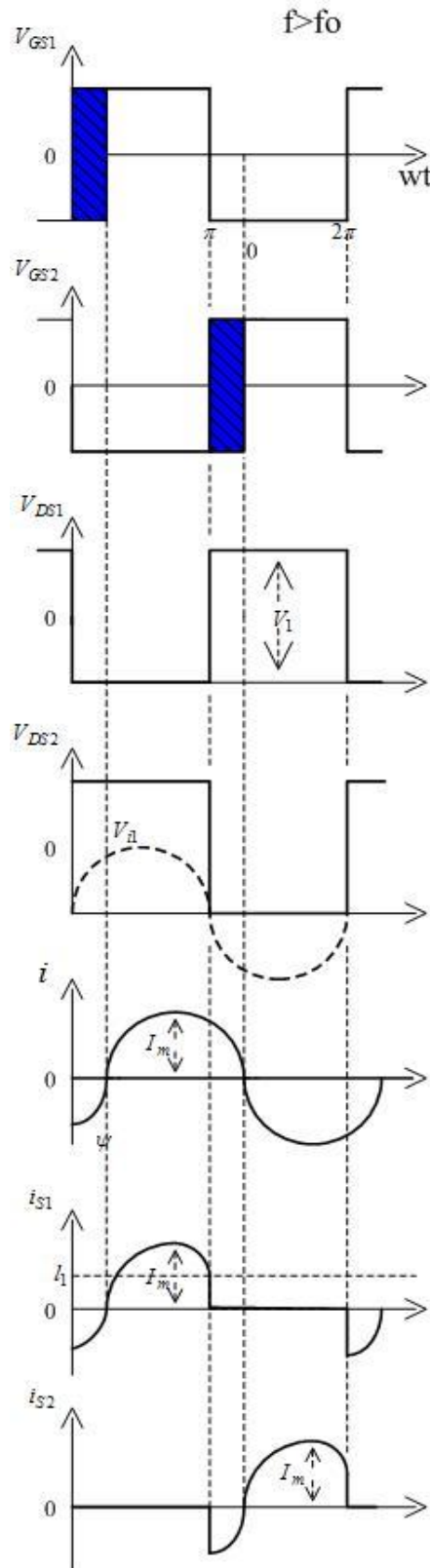


Fig. 3. The key waveforms of the SRPLI under inductive load

Step 3:

To adjust the switching frequency and let the voltage and current of the transducer is in phase. The maximum power point tracking of the proposed system can be achieved.

3. ILLUSTRATION EXAMPLE AND DISCUSSION

An ultrasonic cleaner system with phase control is used to illustrate the previous analysis and design. The equivalent circuit of the transducer is shown in Fig. 4, where the characteristic parameters are listed in Table I. The simulation and measured impedance of the transducer is shown in Fig. 5 (a) and (b). From the simulated and measured results, we can see that the

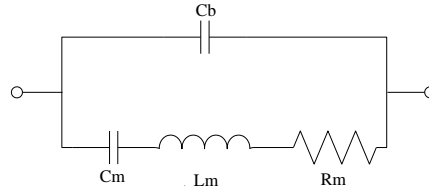
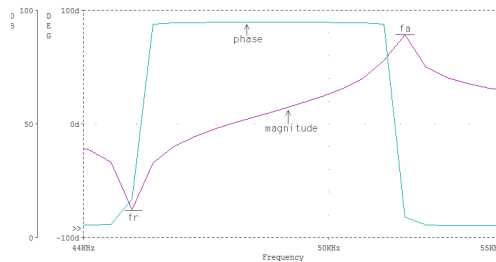
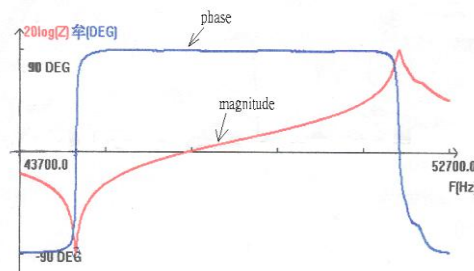


Fig. 4. Equivalent circuit of a piezoelectric transducer



(a)



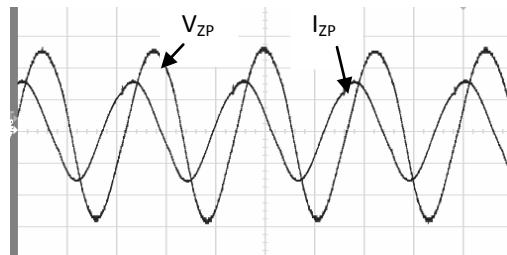
(b)

Fig. 5. Impedance of a piezoelectric transducer: (a) simulation and (b) measured.

The experimental results of the proposed system are shown in Figs. 6-8. Fig. 6(a) shows the measured voltage and current waveforms of the driving system are not in phase without the MPPT control algorithm. With the MPPT control algorithm, we can see that the measured voltage and current waveforms are in phase and shown in Fig. 6(b). Fig. 7 shows the measured voltage V_{DS} and current I_{DS} waveforms of the switch of SRPLI, the ZVS feature is achieved. Fig. 8 shows the measured oscillation waveforms of the piezoelectric transducer for an ultrasonic cleaner. The measured results of the system are shown to verify the MPPT and ZVS features of the proposed system.

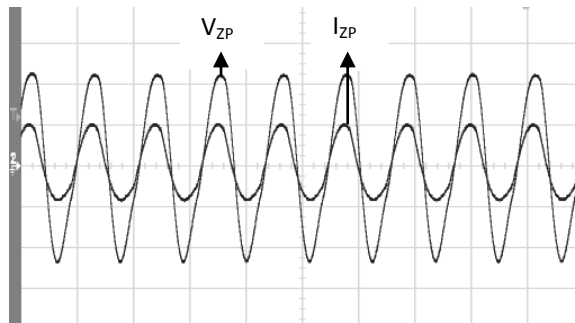
Table I. Characteristic parameters of a piezoelectric transducer

parameters	value
L_m	7.01 mH
C_m	1.79 nF
R_m	1.65 Ω
C_b	5.27 nF
Q	1195.9
f_r	44.89 kHz
f_a	51.66 kHz



($V_{ZP} : 50V/div$ 、 $I_{ZP} : 0.5A/div$ 、time : 20us/div)

(a)



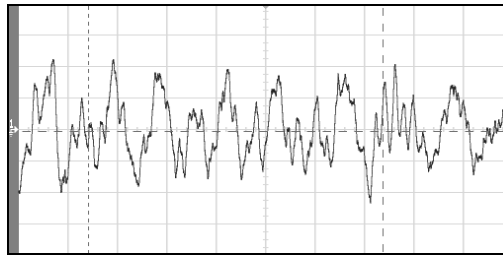
($V_{ZP} : 50V/div$ 、 $I_{ZP} : 0.5A/div$ 、time : 20us/div)

(b)

Fig. 6. Measured voltage V_{ZP} and current I_{ZP} waveforms of the piezoelectric transducer: (a) without MPPT and (b) with MPPT



Fig. 7. Measured voltage V_{DS} and current I_{DS} waveforms of the switches



(V : 2V/div, time : 10us/div)

Fig. 8. Measured oscillation waveforms of the transducer for an ultrasonic cleaner

4. CONCLUSION

This paper proposed a MPPT and ZVS features with a low-cost micro-controller for an ultrasonic cleaner. The design procedure of the proposed piezoelectric transducer system has been outlined in this paper. The prototype of such a piezoelectric transducer system for a 45W ultrasonic cleaner has been designed and implemented. The simulated and measured results of the system are shown to verify the MPPT and ZVS features of the proposed system.

5. ACKNOWLEDGEMENT

This work was supported by the National Science Council, Taiwan, R.O.C., under Projects NSC 102-2221-E-150-025 and NSC 103-3113-E-007-007.

6. REFERENCES

- [1] k. Aqbossou, J.-L. Dion, S. Carignan, M. Abdelkrim and A. Cheriti, "Class D amplifier for a power piezoelectric load," *IEEE Trans. on Ultrasonics, Ferroelectrics and Frequency Control*, vol. 47, July 2000, pp.1036-1041.
- [2] S. S. Muhlen, "Design of an optimized high-power ultrasonic transducer," *IEEE Trans. on Ultrasonics Symposium*, vol.3, Dec 1990, pp.1631-1634.
- [3] J. I. Ishikawa, T. Sato, T. Suzuki, H. Ikeda, H. Yoshida and S. Shinohara, "New type of compact control system for frequency and power in megasonic transducer drive at 1 MHz," in *Proc. Industry Applications Conference*, vol. 3, Oct 1998, pp. 1638-1643
- [4] D. Campolo, M. Sitti and R. S. Fearing, "Efficient charge recovery method for driving piezoelectric actuators with quasi-square waves," *IEEE Trans. on Ultrasonics, Ferroelectrics and Frequency Control*, vol. 50, March 2003, pp. 237-244.
- [5] P. Fabijanski and R. Lagoda, "Series resonant converter with sandwich-type piezoelectric ceramic transducers" in *Proc. ICIT'96*, pp. 252-256.
- [6] C. Kauczor, and N. Frohliche, "Inverter topologies for Ultrasonic Piezoelectric Transducers with High Mechanical Q-Factor" in *Proc. PESC'04*, pp. 2736-2741.
- [7] G. Ivensky, I. Zafrany, and S. Ben-Yaakov, "Generic operational characteristics of piezoelectric transformers," in *Proc. PESC'00*, vol. 3, pp. 1657-1662.
- [8] H.-L. Cheng, C.-A. Cheng, C.-C. Fang, and H.-C. Yen, "Single-Switch High-Power-Factor Inverter Driving Piezoelectric Ceramic Transducer for Ultrasonic cleaner," *IEEE Trans. on Power Electronics*, vol. 58, July 2011, pp. 2898-2905.
- [9] G. Winter, C. Auvigne and Y. Perriard, "Design of a Resonant Power Inverter for a Piezoelectric Actuator," in *Proc. IECON 2012*, pp. 345-349.
- [10] R. A. Pentz, J. Wheeler, G. D. Jager, and R. H. Wilkinson, "Driving an Ultrasonic Transducer with a Multicell Inverter," in *Proc. ECCE-Asia 2013*, pp. 976-980.